

The Dynamical Power Corrections In Hadronic B Decays

Tsung-Wen Yeh*

Department of Nature Science Education, National Taichung University, Taichung 403, Taiwan

We investigate the subleading power suppressed corrections arising from the three parton Fock state of the final state pseudoscalar light mesons in the hadronic B decays. The three parton contributions are evaluated up to $O(\alpha_s^2)$ and $O(1/m_b)$. Our result shows that the three parton contributions play an important role in the understanding of the penguin dominant processes, while have little effects for the tree dominant processes.

PACS numbers: 12.38.Bx, 14.40.-n

Recent years, many rare hadronic decays of B mesons are accessible. They are helpful in studies of CP violations and new physics beyond the standard model. In order to understand these rare processes, the QCD factorization [1, 2] and the PQCD factorization [3, 4, 5] based on QCD and perturbation theory have been investigated extensively. In this work, we would like to employ the QCD factorization to evaluate the three parton contributions.

In the heavy quark mass limit, the QCD factorization demonstrates that the three body matrix element of the effective Hamiltonian could be expressed in terms of a factorization form, in which the short and long distance strong interactions are written as separately incoherent functions. However, it has been noticed that the factorization property maybe invalidate at the twist-3 order [1]. In phenomenology, it was also noticed that the power suppressed corrections may be as important as the radiative corrections [6, 7]. This implies that the extension of QCD factorization to subleading twist order would be important in both theory and phenomenology. Since the sources of higher twist corrections are very complicate and the generalization of leading twist factorization has not been well understood, it is still lacking a systematical method for this extension.

Some kinds of higher twist quantities have been considered, for example, the spin mismatching between the Fock state and the parent meson [8], the higher Fock states [8], the final state interactions [9, 10, 11], the soft gluon corrections [1], the annihilation corrections [1], the spectator corrections [1], and the infrared renormalon corrections [12].

To deal with the above power suppressed quantities may require further assumptions beyond QCD factorization, such as QCD sum rule [1], parton hadron duality for exclusive processes [9, 10, 11], and phenomenological models [1]. However, it is more interesting to evaluate the corrections within the factorization. In this work, we will employ the collinear expansion [13] to calculate the contributions with the three parton $q\bar{q}g$ Fock state of the final state pseudoscalar mesons. The employed expansion method was firstly established in deep inelastic scattering processes [14, 15, 16] and Drell-Yan processes [17]. Lately, the expansion method was generalized for exclusive hard processes [18, 19, 20].

One motivation of this work is to complete the studies of twist-3 power suppressed corrections. The twist-3 corrections contain two parton and three parton contributions, while the later contributions were completely ignored in previous studies [1, 2]. The other motivation concerns that the predictions [2] of QCD factorization for the branching ratios of the penguin dominant $B \rightarrow \pi K$ processes are lower than the new data (see Table III). It is therefore interesting to see whether the neglected three parton contributions can improve the situation. In order to arrive at the same precision order as the two parton contributions, the three parton contributions will be evaluated up to one loop order. The relevant correctional terms are then collected into corresponding parameterization functions for the decay amplitudes, and then applied to make predictions for the branching ratios and the direct CP asymmetries of $B \rightarrow \pi K, \pi\pi$ processes.

At tree level, the $q\bar{q}g$ Fock state of M_2 in the $B \rightarrow M_1 M_2$ decay contributes through the $-2(S - P) \otimes (S + P)$ operators, Q_6 and Q_8 . Its result as combined with the other two parton contributions of the same twist order appears as

$$\langle M_1 M_2 | Q_{6(8)} | B \rangle = c_Q (1 + A_{M_2}^{G_3}) r_X^{M_2} A_{M_1 M_2}, \quad (1)$$

where $c_Q = 1$ for Q_6 and $c_Q = 3e_Q/2$ for Q_8 . The tree function $A_{M_2}^{G_3}$ and the following one loop functions $V_{M_2,3}$, $P_{M_2,3}^{p,(EW)}$ and $A_{3,G_3}^{i(f)}$ are evaluated in the covariant gauge, $\partial \cdot A = 0$. $A_{M_2}^{G_3}$ represents the three parton corrections from

*Electronic address: twyeh@ms3.ntcu.edu.tw

the tree level diagrams as depicted in Fig. 1(a) and 1(b)

$$A_{M_2}^{G_3} = 2 \int [d\alpha] \delta(1 - \Sigma\alpha) \frac{T_{M_2}(\alpha_{\bar{q}_2}, \alpha_{q_1}, \alpha_g)}{\alpha_{q_1} \alpha_g}, \quad (2)$$

where $A_{M_1 M_2} = i(M_B^2 - m_{M_2}^2) F_0^{B \rightarrow M_1} (m_{M_2}^2) f_{M_2}$, and $r_{\chi}^{M_2} = 2m_{M_2}^2 / [\bar{m}_b(\bar{m}_{q_1} + \bar{m}_{q_2})]$. The integral measure $[d\alpha]$ denotes $d\alpha_{\bar{q}_2} d\alpha_{q_1} d\alpha_g$. The three parton distribution amplitude $T_{M_2}(\alpha_{\bar{q}_2}, \alpha_{q_1}, \alpha_g)$ parameterizes the matrix element $\langle M_2 | \bar{q}_1(x) \sigma^{\alpha\beta} \gamma_5 g G^{\mu\nu}(y) q_2(0) | 0 \rangle$ and has a parameterization form $T(\alpha_{\bar{q}_2}, \alpha_{q_1}, \alpha_g) = 360\eta\alpha_{\bar{q}_2}\alpha_{q_1}\alpha_g^2(1 + \omega/2(7\alpha_g - 3))$ [8]. The cross vertices in the diagrams of Fig. 1 and 2 denote $i\gamma_\mu$, which comes from a collinear expansion for the propagators in the diagrams (see below explanations for its definition). The contributions from diagrams Fig. 1(c) and (d) are associated with the octet $(V - A)(V \pm A)$ operators. The related three parton distribution amplitude of M_2 is of twist-4, and relates to the matrix element $\langle M_2 | \bar{q}_1(x) \gamma^\alpha \gamma_5 G^{\mu\nu}(y) q_2(0) | 0 \rangle$ [8]. The associated contributions approximately vanish in the G-parity symmetry [13].

We now briefly describe how the employed collinear expansion is performed in the calculations. The detailed tree level calculations for Fig. 1 refer to [13] and the detailed one loop calculations for Fig. 2 are left to other work [22]. After some manipulations, the expressions for the amplitudes of the Feynman diagrams in Fig. 1 and 2 always involve one convolution integration over the loop parton momenta l_{q_1} and l_g

$$\int \frac{d^4 l_{q_1}}{(2\pi)^4} \int \frac{d^4 l_g}{(2\pi)^4} \text{Tr}[H_\nu(l_{q_1}, l_g) \phi^\nu(l_{q_1}, l_g)], \quad (3)$$

where $H_\nu(l_{q_1}, l_g)$ [42] represents the partonic amplitude for the relevant diagrams, and $\phi^\nu(l_{q_1}, l_g)$ denotes the amplitude with which the $q\bar{q}g$ state composes of the meson M_2

$$\phi^\nu(l_{q_1}, l_g) = \int d^4 x \int d^4 y e^{il_{q_1} \cdot x} e^{il_g \cdot y} \langle M_2 | \bar{q}_1(x) (-g A^\nu(y)) q_2(0) | 0 \rangle. \quad (4)$$

The trace is taken over fermion and color indices. By making a scale analysis for the loop momenta l_{q_1} and l_g in $H_\nu(l_{q_1}, l_g)$, it is not difficult to find that the dominant contributions should come from the regions in which both l_{q_1} and l_g are collinear to the momentum q of the emitted meson, and the other possible regions are power suppressed by at least one additional order of $1/m_b$. It is followed by making a Taylor expansion for $H_\nu(l_{q_1}, l_g)$ with respect to $\hat{l}_{q_1} = \alpha_{q_1} q$ and $\hat{l}_g = \alpha_g q$ as

$$H_\nu(l_{q_1}, l_g) = H_\nu(\hat{l}_{q_1}, \hat{l}_g) + H_{\mu\nu}(\hat{k})(k - \hat{k})^\mu + \dots, \quad (5)$$

where $H_{\mu\nu}(\hat{k}) = \partial H_\nu(\hat{k}) / \partial k^\mu$ and $k = l_{q_1} + l_g$. The derivative of $H_\nu(k)$ over momentum k^μ introduces the cross vertices in Fig. 1 and 2. The $(k - \hat{k})^\mu$ factor is absorbed by $\phi^\nu(l_{q_1}, l_g)$ to introduce the field strength $G^{\mu\nu}(y)$ in the matrix element $\langle M_2 | \bar{q}_1(x) \sigma^{\alpha\beta} \gamma_5 g G^{\mu\nu}(y) q_2(0) | 0 \rangle$. In covariant gauge, the longitudinal component $n \cdot A q^\nu$ of the gluon field A^ν is dominant with $n \cdot q = 1$. The contraction of H_ν with q^ν vanishes due to the Ward identity. $H_{\mu\nu}(\hat{k})$ can be decomposed as $H_{\mu\nu}(\hat{k}) = A_{\mu\nu}(\hat{k}) g_{\mu\nu} + B_{\mu\nu}(\hat{k}) \sigma_{\mu\nu}$. The $g_{\mu\nu}$ term as contracted with $\phi^\nu(k)$ is reduced to a gauge phase factor of the corresponding two parton function. The contraction of the $\sigma_{\mu\nu}$ term with $(k - \hat{k})^\mu \phi^\nu(k)$ leads to the result. There may arise end point divergences due to the momentum derivatives, which are completely cancelled out by the corresponding numerator factors. The final result is then free from the end point divergences. This fact can be read from the following expressions of the vertex, penguin and annihilation corrections.

For most pseudoscalar mesons, such as π, K and η mesons, the parameters in $T_{M_2}(\alpha_{\bar{q}_2}, \alpha_{q_1}, \alpha_g)$ take the values $\eta = 0.015$ and $\omega = -3$ [8]. It results in that $A_{M_2}^{G_3} = 0.585$. The three parton contributions then enhance the twist-3 corrections by about 50%. This gives about two times enhancement in the predictions of branching ratio for the penguin dominated $B \rightarrow \pi K$ processes. For example, the two parton prediction for the branching ratio $Br(B^- \rightarrow \pi^- \bar{K}^0)$ is equal to 11.4×10^{-6} , while the three parton prediction equal to 23.5×10^{-6} is in agreement with the new world average $(24.1 \pm 1.3) \times 10^{-6}$. The QCD factorization prediction for the same process is 20.3×10^{-6} . For the other penguin dominant processes shown in Table III, one can observe similar effects. This seems to imply that the three parton contributions are significant in the understanding of the penguin dominant processes. One similar observation has been obtained for $B \rightarrow V\gamma$ decay [23].

Up to one loop order of radiative corrections, only coefficient functions $a_{6(8)}^p$, with $p = u, c$, are corrected by the three parton contributions as

$$a_6^p = C_6 + \frac{C_5}{N_C} (1 + V_{M_2,3} \frac{C_F \alpha_s}{4\pi}) + \frac{C_F \alpha_s}{4\pi N_C} P_{M_2,3}^p, \quad (6)$$

$$a_8^p = C_6 + \frac{C_5}{N_C} (1 + V_{M_2,3} \frac{C_F \alpha_s}{4\pi}) + \frac{\alpha}{9\pi N_C} P_{M_2,3}^{p,EW}, \quad (7)$$

where $V_{M_2,3}$ and $P_{M_2,3}^{p,(EW)}$ denote the vertex and penguin one loop radiative corrections, respectively. The quark gluon interaction vertices and the cross vertices are inserted into the diagrams in all possible ways. There are totally 32 vertex diagrams similar to that one depicted in Fig. 2(a). The calculations of 32 vertex diagrams are collected in the function $V_{M_2,3}^{G_3}$ of $V_{M_2,3} = -6 + V_{M_2,3}^{G_3}$, which is expressed as

$$V_{M_2}^{G_3} = -6 \int [d\alpha] T_{M_2}(\alpha_{\bar{q}_2}, \alpha_{q_1}, \alpha_g) \frac{g(\alpha_{\bar{q}_2})}{\alpha_{q_1} \alpha_g} \quad (8)$$

where

$$g(\alpha) = 2\left(\frac{\ln \bar{\alpha}}{\alpha} - \frac{\ln \alpha}{\bar{\alpha}}\right) + (\text{Li}_2(1 - \frac{1}{\alpha}) - \text{Li}_2(1 - \frac{1}{\bar{\alpha}})) + 2(\ln \bar{\alpha} - \ln \alpha) + 2\left(\frac{\alpha}{\bar{\alpha}} \ln \alpha - \frac{\bar{\alpha}}{\alpha} \ln \bar{\alpha}\right). \quad (9)$$

The penguin corrections $P_{M_2,3}^{p,(EW)} = P_{M_2,3}^{p,(EW),2} + P_{M_2,3}^{p,(EW),G_3}$, contain the two parton corrections $P_{M_2,3}^{p,(EW),2}$ [1] and the three parton corrections $P_{M_2,3}^{p,(EW),G_3}$. The functions $P_{M_2,3}^{p,(EW),G_3}$ collecting the calculations of 42 diagrams similar to the one depicted in Fig. 2(b) are expressed

$$P_{M_2,3}^{p,G_3}(\mu) = \left[C_1 \left[2A_{M_2}^{G_3} \left(\ln\left(\frac{m_b}{\mu}\right) - \frac{2}{3} \right) + G_{M_2}^{G_3}(s_p) \right] + C_3 \left[4A_{M_2}^{G_3} \left(\ln\left(\frac{m_b}{\mu}\right) - \frac{2}{3} \right) + G_{M_2}^{G_3}(0) + G_{M_2}^{G_3}(1) \right] \right. \\ \left. + (C_4 + C_6) \left[2n_f A_{M_2}^{G_3} \left(\ln\left(\frac{m_b}{\mu}\right) - \frac{1}{3} \right) + (n_f - 2) G_{M_2}^{G_3}(0) + G_{M_2}^{G_3}(s_c) + G_{M_2}^{G_3}(1) \right] \right], \quad (10)$$

$$P_{M_2,3}^{p,EW,G_3}(\mu) = (C_1 + N_c C_2) \left[2A_{M_2}^{G_3} \left(\ln\left(\frac{m_b}{\mu}\right) - \frac{2}{3} \right) + G_{M_2}^{G_3}(s_p) \right], \quad (11)$$

where

$$G_{M_2}^{G_3}(s) = -3 \int [d\alpha] T_{M_2}(\alpha_{\bar{q}_2}, \alpha_{q_1}, \alpha_g) \frac{G(s, 1 - \alpha_{\bar{q}_2})}{\alpha_{q_1} \alpha_g} \quad (12)$$

, $G(s, x)$ is the penguin function

$$G(s, x) = -4 \int_0^1 du \bar{u} u \ln[s - u \bar{u} x] \quad (13)$$

, and $s_p = (m_p/m_b)^2$ with $p = u, c$.

The three parton corrections for the annihilation diagrams are collected into $A_{3,G_3}^{i(f)}(\mu)$ in $A_3^{i(f)}(\mu) = A_{3,2}^{i(f)}(\mu) + A_{3,G_3}^{i(f)}(\mu)$. $A_{3,2}^{i(f)}(\mu)$ denotes the twist-3 two parton annihilation function. The function $A_3^{i(f)}(\mu)$ is much smaller than the function $A_3^f(\mu)$ at the scale $\mu = m_b$ and will be neglected in our calculations. Collecting calculations of 48 annihilation diagrams, we obtains

$$A_{3,G_3}^f(\mu) = 6\pi\alpha_s(\mu) r_\chi^{M_i} \int_0^1 dx \int_0^1 dy \left[\delta_{M_1}^{M_i} \delta(y - \alpha_{\bar{q}_2}) \phi_{M_2}(x) + \delta_{M_2}^{M_i} \delta(\bar{x} - \alpha_{\bar{q}_2}) \phi_{M_1}(y) \right] \int [d\alpha] \frac{T_{M_i}(\alpha_{\bar{q}_2}, \alpha_{q_1}, \alpha_g)}{\bar{x} y \alpha_{q_1} \alpha_g} \\ \approx \left(\frac{9}{80} \right) \times 6\pi\alpha_s(\mu) (r_\chi^{M_1} + r_\chi^{M_2}). \quad (14)$$

It is noted that A_{3,G_3} is free from end-point divergence. A_{3,G_3}^f is only 1.5% of $A_{3,2}^f$ and can be neglected for practics.

The factorization scale has been chosen to be m_b in the following phenomenological analysis. The input parameters are listed in Table I [2]. The decay amplitudes are expressed in terms of a_i^p (containing Wilson coefficients, vertex, penguin and hard spectator corrections), $b_j^{p,(EW)}$ (containing annihilation corrections), and $A_{M_1 M_2}$, in which $i = 1, \dots, 10$, $j = 1, \dots, 4$, $p = u, c$, and $M_1 M_2 = \pi K, \pi\pi$. The definitions of a_i^p and $b_j^{p,(EW)}$ refer to [1]. Since the twist-3 three parton annihilation corrections can be completely neglected, we have employed the evaluated values of $b_i^{p,(EW)}$ at the scale $\sqrt{\Lambda_h m_b}$ with $\Lambda_h = 0.5$ GeV in [1]. The relevant Wilson coefficients $C_i(\mu)$, $i = 1, \dots, 10$, are evaluated in Table II by employing the NLO formula [24, 25, 26, 27]. It is noted that the evaluated values of $C_i(\mu)$, $i = 1, \dots, 10$ in Table II are in agreement with [1, 27]. To benefit future studies, we have also included the values of $C_i(\mu)$ evaluated at six relevant scales $\mu = 2m_b, m_b, m_b/2, \sqrt{2\Lambda_h m_b}, \sqrt{\Lambda_h m_b}, \sqrt{\Lambda_h m_b}/2$ in Table II.

We now apply the above calculations to make predictions for CP-averaged branching ratios, and for direct CP asymmetries, under " \bar{B} minus B " convention, for $B \rightarrow \pi K$ and $B \rightarrow \pi\pi$ decays. The predicted CP-averaged branching ratios and direct CP asymmetries are listed in Table III. The most recent measurements by BaBar[28, 29, 30, 31, 32, 33], Belle [34, 35, 36], CLEO [37, 38, 39], and CDF [40] experiments, and the world averages derived by HFAG group [41] are shown. For comparison, the predictions made in [2] are adopted.

For penguin dominant $B \rightarrow \pi K$ processes, it is shown that the three parton effects are significant in understanding these processes. The predicted branching ratios with three parton corrections (the column II) are close to the experimental data, while the predicted branching ratios without three parton corrections (the column I) are much lower than the data. There are about two times enhancements of the three parton branching ratio predictions over the two parton predictions. At the amplitude level, the tree level and the one loop three parton corrections enhance the twist-3 contributions by 50% and 15%, respectively.

Our two parton branching ratio predictions (the first column) are smaller than those predictions from [2] (the third column), by a factor about $1.6 \sim 1.7$. In order to check this difference, we have repeated the calculations made in [2] to evaluate the two parton branching ratios, by employing the evaluated values for a_i^p and $b_j^{(EW)}$ and the same input parameters. We found that the evaluated two parton branching ratio predictions are very close to our two parton predictions by only a few percent differences. Due to insufficient informations about how the predictions of [2] could be obtained, we can not identify the sources of this difference.

For tree dominant $B \rightarrow \pi\pi$ processes, twist-3 three parton contributions have small effects as expected. The predicted two parton and three parton branching ratios are very close to each other, and are in consistent with the predictions of [2]. It is noted that the three parton branching ratio prediction for $\bar{B}^0 \rightarrow \pi^0\pi^0$ is equal to 1.1×10^{-6} in agreement with the data $(1.45 \pm 0.29) \times 10^{-6}$. For reference, the two parton prediction is 0.7×10^{-6} (c.f. 0.3×10^{-6} [2]). Except of $\bar{B}^0 \rightarrow \pi^+\pi^-$ mode, our three parton predictions agree with the data. However, as noted in [2], it is possible to tune the prediction for the branching ratio of $\bar{B}^0 \rightarrow \pi^+\pi^-$ to be consistent with the data within some parameter spaces (the scenario S_4). To show this fact, we also list the predictions under the scenario S_4 in the paragraph in the third column of Table. III.

Due to large uncertainties in the experimental data of direct CP asymmetries of $B \rightarrow \pi K, \pi\pi$ decays, it is still difficult to reach a solid conclusion for theoretical predictions. The most certain measurement $A_{CP}(\bar{B}^0 \rightarrow \pi^- K^+) = -10.9 \pm 1.9$ has a different sign and a larger magnitude than our two parton and three parton predictions. Our three parton predictions for $A_{CP}(B^- \rightarrow \pi^- K^0)$ and $A_{CP}(\bar{B}^0 \rightarrow \pi^0 \bar{K}^0)$ has changed the sign of the corresponding two parton predictions to be the same signs of the data.

In this work, we have employed the collinear expansion and QCD factorization to evaluate the decay amplitudes of B mesons into two pseudoscalar mesons up to $O(\alpha_s^2)$ and $O(1/m_b)$. The calculations are applied to make predictions for the CP-averaged branching ratios and direct CP asymmetries of $B \rightarrow \pi K, \pi\pi$ processes. Our analysis indicates that the twist-3 three parton corrections play an important role in the understanding of penguin dominant $B \rightarrow \pi K$ processes.

Acknowledgements The author thanks D. Pirjol and H.N. Li for useful discussions. The author appreciates partial financial support from the National Science Council under grand numbers NSC-93-2112-M-142-001 and NSC-94-2112-M-142-001.

-
- [1] M. Beneke, G. Buchalla, M. Neubert and C. T. Sachrajda, Nucl. Phys. B **606**, 245 (2001) [arXiv:hep-ph/0104110].
 - [2] M. Beneke and M. Neubert, Nucl. Phys. B **675**, 333 (2003) [arXiv:hep-ph/0308039].
 - [3] T. W. Yeh and H. n. Li, Phys. Rev. D **56**, 1615 (1997) [arXiv:hep-ph/9701233].
 - [4] Y. Y. Keum, H. N. Li and A. I. Sanda, Phys. Rev. D **63**, 054008 (2001) [arXiv:hep-ph/0004173].
 - [5] Y. Y. Keum, H. n. Li and A. I. Sanda, Phys. Lett. B **504**, 6 (2001) [arXiv:hep-ph/0004004].
 - [6] N. de Groot, W. N. Cottingham and I. B. Whittingham, Phys. Rev. D **68**, 113005 (2003) [arXiv:hep-ph/0308269].
 - [7] T. N. Pham and G. Zhu, Phys. Rev. D **69**, 114016 (2004) [arXiv:hep-ph/0403213].
 - [8] P. Ball, JHEP **9901**, 010 (1999) [arXiv:hep-ph/9812375].
 - [9] Z. z. L. Xing, Phys. Lett. B **493**, 301 (2000) [arXiv:hep-ph/0007136].
 - [10] P. Zenczykowski, Phys. Rev. D **63**, 014016 (2001) [arXiv:hep-ph/0009054].
 - [11] K. Terasaki, Int. J. Theor. Phys. Group Theor. Nonlin. Opt. **8**, 55 (2002) [arXiv:hep-ph/0011358].
 - [12] M. Neubert and B. D. Pecjak, JHEP **0202**, 028 (2002) [arXiv:hep-ph/0202128].
 - [13] T. W. Yeh, arXiv:hep-ph/0210272.
 - [14] R. K. Ellis, W. Furmanski and R. Petronzio, Nucl. Phys. B **207**, 1 (1982).
 - [15] R. K. Ellis, W. Furmanski and R. Petronzio, Nucl. Phys. B **212**, 29 (1983).
 - [16] J. W. Qiu, Phys. Rev. D **42**, 30 (1990).
 - [17] J. w. Qiu and G. Sterman, Nucl. Phys. B **353**, 105 (1991).
 - [18] T. W. Yeh, arXiv:hep-ph/0107018.

- [19] T. W. Yeh, Phys. Rev. D **65**, 074016 (2002) [arXiv:hep-ph/0107192].
- [20] T. W. Yeh, Phys. Rev. D **65**, 094019 (2002) [arXiv:hep-ph/0204264].
- [21] T. W. Yeh, Phys. Rev. D **66**, 014002 (2002).
- [22] T. W. Yeh, in preparation.
- [23] A. Hardmeier, E. Lunghi, D. Pirjol and D. Wyler, Nucl. Phys. B **682**, 150 (2004) [arXiv:hep-ph/0307171].
- [24] A. J. Buras, M. Jamin and M. E. Lautenbacher, Nucl. Phys. B **400**, 75 (1993) [arXiv:hep-ph/9211321].
- [25] M. Ciuchini, E. Franco, G. Martinelli and L. Reina, Phys. Lett. B **301**, 263 (1993) [arXiv:hep-ph/9212203].
- [26] M. Ciuchini, E. Franco, G. Martinelli and L. Reina, Nucl. Phys. B **415**, 403 (1994) [arXiv:hep-ph/9304257].
- [27] G. Buchalla, A. J. Buras and M. E. Lautenbacher, Rev. Mod. Phys. **68**, 1125 (1996) [arXiv:hep-ph/9512380].
- [28] B. Aubert *et al.* [BABAR Collaboration], Phys. Rev. Lett. **92**, 201802 (2004) [arXiv:hep-ex/0312055].
- [29] B. Aubert *et al.* [BABAR Collaboration], Phys. Rev. Lett. **94**, 181802 (2005) [arXiv:hep-ex/0412037].
- [30] B. Aubert *et al.* [BaBar Collaboration], Phys. Rev. Lett. **93**, 131801 (2004) [arXiv:hep-ex/0407057].
- [31] B. Aubert *et al.* [BABAR Collaboration], arXiv:hep-ex/0408080.
- [32] B. Aubert *et al.* [BABAR Collaboration], Babar-CONF-05/13 (LepPho05 contributed paper).
- [33] B. Aubert *et al.* [BABAR Collaboration], Phys. Rev. D **71**, 111102 (2005) [arXiv:hep-ex/0503011].
- [34] Y. Chao *et al.* [Belle Collaboration], Phys. Rev. D **69**, 111102 (2004) [arXiv:hep-ex/0311061].
- [35] Y. Chao *et al.* [BELLE Collaboration], Phys. Rev. D **71**, 031502 (2005) [arXiv:hep-ex/0407025].
- [36] K. Abe *et al.* [Belle Collaboration], Phys. Rev. Lett. **94**, 181803 (2005) [arXiv:hep-ex/0408101].
- [37] A. Bornheim *et al.* [CLEO Collaboration], Phys. Rev. D **68**, 052002 (2003) [arXiv:hep-ex/0302026].
- [38] S. Chen *et al.* [CLEO Collaboration], Phys. Rev. Lett. **85**, 525 (2000) [arXiv:hep-ex/0001009].
- [39] K. Abe *et al.* [CLEO Collaboration], arXiv:hep-ex/0507045.
- [40] A. Warburton [CDF Collaboration], Int. J. Mod. Phys. A **20**, 3554 (2005) [arXiv:hep-ex/0411079].
- [41] H. F. A. Group, arXiv:hep-ex/0505100.
- [42] Only loop parton momenta are shown in the function H_ν . The radiative loop momentum dependence is implied for the amplitudes of Fig. 2.

$\Lambda_{MS}^{(5)}$	$m_b(m_b)$	$m_c(m_b)$	$m_s(2 \text{ GeV})$
0.225 GeV	4.2 GeV	1.3 GeV	0.090 GeV
$ V_{cb} $	$ V_{ub}/V_{cb} $	γ	$\tau(B^-)$
0.041	0.09	$(70 \pm 20)^\circ$	1.67(ps)
$\tau(B_d)$	f_π	f_K	f_B
1.54(ps)	131 MeV	160 MeV	200 MeV
$F_0^{B \rightarrow \pi}$	$F_0^{B \rightarrow K}$	α_2^π	$\alpha_1^{\bar{K}}$
0.28	0.34	0.1	0.2
$\alpha_2^{\bar{K}}$	λ_B	η	ω
0.1	350 MeV	0.015	-3.0

TABLE I: Input parameters for numerical calculations. Only central values of parameters are used.

C_i	$\sqrt{\Lambda_h m_b}/2$	$\sqrt{\Lambda_h m_b}$	$\sqrt{2\Lambda_h m_b}$	$m_b/2$	m_b	$2m_b$
C_1	1.251	1.190	1.146	1.144	1.086	1.047
$-C_2$	0.468	0.373	0.301	0.297	0.191	0.113
C_3	350	268	212	209	136	88
$-C_4$	761	615	510	504	354	246
C_5	120	124	118	118	98.4	76.6
$-C_6$	1157	862	673	662	427	279
$-C_7$	0.489	0.984	1.000	0.989	0.159	-1.384
C_8	14.2	10.3	7.82	7.68	4.81	3.086
$-C_9$	111	107	103	103	97.6	93.1
C_{10}	41.6	33.5	28.1	27.7	19.4	12.9

TABLE II: The Wilson coefficients $C_i(\mu)$, $i = 1, \dots, 10$ are evaluated at scales $\mu = \sqrt{\Lambda_h m_b}/2, \sqrt{\Lambda_h m_b}, \sqrt{\Lambda_h 2m_b}, m_b/2, m_b, 2m_b$, with $\Lambda_h = 0.5 \text{ GeV}$. The values of C_{3-10} are in units of 10^{-4} .

Br	I	II	[2]	BaBar	Belle	CLEO	average
$B^- \rightarrow \pi^- K^0$	$11.4^{+0.2}_{-0.1}$	$23.5^{+0.2}_{-0.3}$	$19.3^{+1.9}_{-0.3} (20.3)$	$26.0 \pm 1.3 \pm 1.0$	$22.0 \pm 1.9 \pm 1.1$	$18.8^{+3.7+2.1}_{-3.3-1.8}$	24.1 ± 1.3
$B^- \rightarrow \pi^0 K^-$	$6.2^{+1.0}_{-0.8}$	$12.3^{+1.3}_{-1.2}$	$11.1^{+1.8}_{-1.7} (11.7)$	$12.0 \pm 0.7 \pm 0.6$	$12.0 \pm 1.3^{+1.3}_{-0.9}$	$12.9^{+2.4+1.2}_{-2.2-1.1}$	12.1 ± 0.8
$\bar{B}^0 \rightarrow \pi^+ K^-$	$9.7^{+1.4}_{-1.2}$	$20.2^{+1.9}_{-1.8}$	$16.3^{+2.6}_{-1.7} (18.4)$	$17.9 \pm 0.9 \pm 0.7$	$18.5 \pm 1.0 \pm 0.7$	$18.0^{+2.3+1.2}_{-2.1-0.9}$	18.2 ± 0.8
$\bar{B}^0 \rightarrow \pi^0 \bar{K}^0$	$4.5^{+0.1}_{-0.2}$	$9.7^{+0.2}_{-0.3}$	$7.0^{+0.7}_{-0.7} (8.0)$	$11.4 \pm 0.9 \pm 0.6$	$11.7 \pm 2.3^{+1.2}_{-1.3}$	$12.8^{+4.0+1.7}_{-3.3-1.4}$	11.5 ± 1.0
$\bar{B}^0 \rightarrow \pi^+ \pi^-$	$7.8^{+0.9}_{-1.1}$	$7.9^{+1.3}_{-1.4}$	$8.9^{+4.0}_{-3.4} (5.2)$	$4.7 \pm 0.6 \pm 0.2$	$4.4 \pm 0.6 \pm 0.3$	$4.5^{+1.4+0.5}_{-1.2-0.4}$	4.5 ± 0.4
$B^- \rightarrow \pi^- \pi^0$	$5.9^{+0.1}_{-0.1}$	$5.9^{+0.1}_{-0.1}$	$6.0^{+3.0}_{-2.4} (5.1)$	$5.8 \pm 0.6 \pm 0.4$	$5.0 \pm 1.2 \pm 0.5$	$4.6^{+1.8+0.6}_{-1.6-0.7}$	5.5 ± 0.6
$\bar{B}^0 \rightarrow \pi^0 \pi^0$	$0.7^{+0.2}_{-0.3}$	$1.1^{+0.5}_{-0.4}$	$0.3^{+0.2}_{-0.2} (0.7)$	$1.17 \pm 0.32 \pm 0.10$	$2.3^{+0.4+0.2}_{-0.5-0.3}$	< 4.4	1.45 ± 0.29
A_{CP}	I	II	[2]	BaBar	Belle	CLEO	average
$B^- \rightarrow \pi^- K^0$	$0.2^{+0.0}_{-0.1}$	$-0.7^{+0.1}_{-0.0}$	$0.9^{+0.2}_{-0.3} (0.3)$	$-8.7 \pm 4.6 \pm 1.0$	$5.0 \pm 5.0 \pm 1.0$	$18 \pm 24 \pm 2$	-2.0 ± 3.4
$B^- \rightarrow \pi^0 K^-$	$19.0^{+0.0}_{-1.4}$	$8.7^{+0.0}_{-0.9}$	$7.1^{+1.7}_{-1.8} (-3.6)$	$6 \pm 6 \pm 1$	$4 \pm 5 \pm 2$	$-29 \pm 23 \pm 2$	4 ± 4
$\bar{B}^0 \rightarrow \pi^+ K^-$	$15.8^{+0.0}_{-1.1}$	$5.9^{+0.0}_{-0.7}$	$4.5^{+1.1}_{-1.1} (-4.1)$	$-13.3 \pm 3.0 \pm 0.9$	$-10.1 \pm 2.5 \pm 0.5$	$-4 \pm 16 \pm 2$	-10.9 ± 1.9
$\bar{B}^0 \rightarrow \pi^0 \bar{K}^0$	$-6.6^{+1.4}_{-0.6}$	$4.6^{+1.0}_{-0.4}$	$-3.3^{+1.0}_{-0.8} (0.8)$	$6 \pm 18 \pm 3$	$12 \pm 20 \pm 7$		9 ± 14
$\bar{B}^0 \rightarrow \pi^+ \pi^-$	$-13.7^{+3.7}_{-3.2}$	$-10.1^{+3.0}_{-2.1}$	$-6.5^{+2.1}_{-2.1} (10.3)$	$-9 \pm 15 \pm 4$	$-56 \pm 12 \pm 6$		-37 ± 10
$B^- \rightarrow \pi^- \pi^0$	0.0	0.01	$-0.02^{+0.01}_{-0.01} (-0.02)$	$-1 \pm 10 \pm 2$	$-2 \pm 10 \pm 1$		-2 ± 7
$\bar{B}^0 \rightarrow \pi^0 \pi^0$	$68.2^{+13.9}_{-15.1}$	$60.6^{+19.4}_{-15.6}$	$45.1^{+18.4}_{-12.8} (-19.0)$	$12 \pm 56 \pm 6$	$44^{+53}_{-52} \pm 17$		28^{+40}_{-39}

TABLE III: The column I and II are predictions without and with including three parton corrections, respectively. The branching ratios are in units of 10^{-6} and the CP asymmetries in units of 10^{-2} . The errors for predictions in column I and II correspond to $\gamma = (70 \pm 20)^\circ$. The combination of uncertainties in V_{ub}, V_{cb} and γ refers to the errors in the third column. The experimental data are adopted from BaBar, Belle, CLEO experiments. The world average are obtained from the HFAG group.

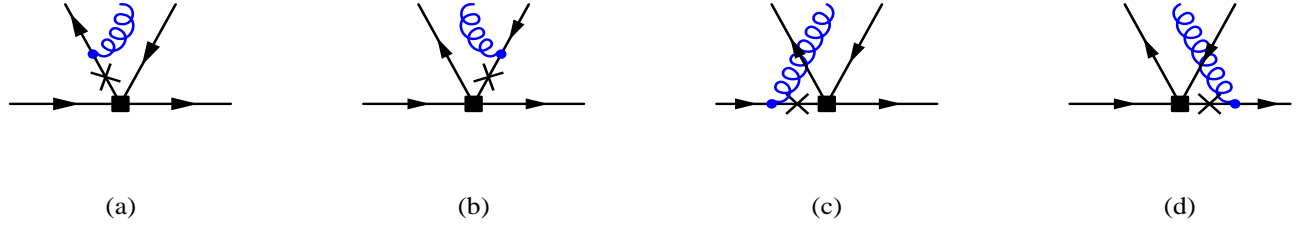


FIG. 1: The one gluon insertion diagrams for $B \rightarrow P_1 P_2$. The square symbol represents the vertex of weak interactions. The explanation of the cross vertex refers to the text.

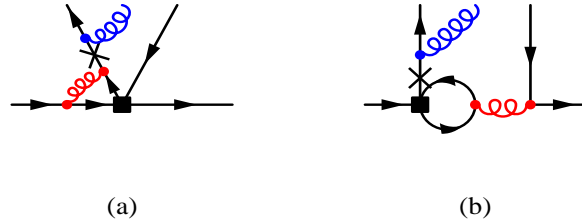


FIG. 2: The vertex and penguin diagrams with one gluon insertion. The square symbol represents the vertex of weak interactions. The explanation of the cross vertex refers to the text.